Raindrop Size Distribution and Radar Parameters in Coastal Tropical Rain Systems of Northeastern Brazil

RICARDO SARMENTO TENÓRIO

Instituto de Ciências Atmosféricas, Universidade Federal de Alagoas, Maceió, Alagoas, Brazil

MARCIA CRISTINA DA SILVA MORAES

Departamento de Meteorologia, Universidade Federal de Campina Grande, Campina Grande, Paraíba, Brazil

HENRI SAUVAGEOT

Laboratoire d'Aérologie, Observatoire Midi-Pyrénées, Université Paul Sabatier—Toulouse III, Toulouse, France

(Manuscript received 17 June 2011, in final form 13 March 2012)

ABSTRACT

A dataset on raindrop size distribution (DSD) gathered in a coastal site of the Alagoas state in northeastern Brazil is used to analyze some differences between continental and maritime rainfall parameters. The dataset is divided into two subsets. One is composed of rainfall systems coming from the continent and moving eastward (i.e., offshore), representing the continental subset. The other is composed of rainfall systems that developed over the sea and are moving westward (i.e., inshore), representing the maritime subset. The mean conditional rain rate (i.e., for rain rate $R > 0$) is found to be higher for maritime (4.6 mm h^{-1}) than for continental (3.2 mm h^{-1}) conditions. The coefficient of variation of the conditional rain rate is lower for the maritime (1.75) than for the continental (2.25) subset. The continental and maritime DSDs display significant differences. For drop diameter D smaller than about 2 mm, the number of drops is higher for maritime rain than for continental rain. This reverses for $D > 2$ mm, in such a way that radar reflectivity factor Z for the maritime case is lower than for the continental case at the same rain rate. These results show that, to estimate precipitation by radar in the coastal area of northeastern Brazil, coefficients of the Z–R relation need to be adapted to the direction of motion of the rain-bearing system, inshore or offshore.

1. Introduction

Rain-system observations from ground-based radar and satellite demonstrate that the physics and dynamics of storms located over land and over oceans present some significant differences that are linked to dynamic causes. A remarkable illustration, suggesting that the severity of storms over land is stronger than over sea, is provided by the global frequency distribution of lightning observed from space (Orville and Henderson 1986; Christian et al. 2003). From ground-based Doppler radar data on continental and oceanic convective storms observed in Oklahoma and in the Darwin area of Australia, Zipser and Lutz (1994) found that, for midlatitude and tropical continental convective storms, radar reflectivity exhibits a maximum somewhat above the surface and displays a gradual decrease with height above freezing level. In sharp contrast, in tropical oceanic storms, the reflectivity vertical profile displays its maximum at the lowest level and experiences a very rapid decrease with height, beginning just above freezing level. Correlatively, updraft velocities in tropical convective cells are much weaker over sea than over land. Yet the strongest and best quantitative evidence about land and ocean convective storm structure differences was provided by the Tropical Rainfall Measuring Mission (TRMM; e.g., Kummerow et al. 1998) data from the combination of high-resolution radar reflectivity profiles with passive microwave, infrared, and lightning

Corresponding author address: Prof. Dr. Ricardo Sarmento Tenório, Sistema de Radar Meteorológico, ICAT, Universidade Federal de Alagoas, Cidade Universitária, Tabuleiro do Martins, Maceió, Alagoas 57072-970, Brazil.
E-mail: ricardo.sarmento@pq.cnpq.br

DOI: 10.1175/JAMC-D-11-0121.1

data (Nesbitt and Zipser 2003; Liu and Zipser 2005; Zipser et al. 2006; Gebremichael et al. 2008; Liu et al. 2008, among others). Results from TRMM data confirm that land storms tend to have a higher reflectivity and reach a higher altitude than do oceanic storms. The horizontal size of oceanic storms decreases with altitude. For oceanic storms, reflectivity above freezing level decreases more rapidly with altitude than for land storms and updraft velocities are much weaker in oceanic storms than in land storms. As a result, above freezing level, near-complete glaciation, a near absence of large ice particles, a large concentration of small ice particles, and low lightning activity are characteristic of oceanic convective cells, as first emphasized by Black and Halett (1986) from observations in hurricane clouds. Differences between land and oceanic storms also concern the frequency of occurrence, the relation between storm intensity and rainfall production, and the diurnal cycle, with a strong afternoon maximum over land and a broad, low-amplitude nocturnal maximum over oceans. All of that shows that land–ocean differences of storm activity and rainfall production are not simple and homogeneous over the earth. Global distributions of storm activity (Orville and Henderson 1986; Christian et al. 2003) notably show that land–ocean differences do not follow exactly the geographic (coastal) contours of continents. In particular, the storm activity distribution is strongly affected by coast shape, presence of mountain ranges, and direction of the general circulation with respect to shoreline orientation. See, for example, the distribution at the transition for the west- and east-coastal areas of tropical Africa or of tropical South America in Figs. 3, 6, 7, and 8 of Zipser et al. (2006). It is notably obvious that, in the presence of inshore circulation through a north–south-oriented coast, the weaker storm intensity of maritime convection is advected inland over some distance. In the presence of an offshore circulation, the transition is more abrupt, with the continental character reaching the coastline with full intensity and decreasing rapidly over sea [e.g., the west coast of tropical Africa in Fig. 3 of Zipser et al. (2006); see also Seity et al. 2000, 2001; Nzeukou and Sauvageot 2002; Sall and Sauvageot 2005; Sall et al. 2006; Nzeukou et al. 2006]. These regional differences at the land–sea transition are not well documented. In particular, what is the influence of these land–ocean or ocean–land transitions on the rain microstructure and on radar parameters?

The main observable that can be used to characterize and describe the rainfall production by cloud systems is the raindrop size distribution (DSD) from which most rainfall and radar parameters can be inferred. The relation between the dynamic structure of cloud systems and DSD has been illustrated and discussed in numerous papers (e.g., Yuter and Houze 1997; Atlas et al. 1999; Tokay et al. 1999; Atlas et al. 2000; Nzeukou et al. 2004; Lee and Zawadzki 2005; Munchak and Tokay 2008, among others). Instantaneous DSDs—that is, at the time step of disdrometer observation (e.g., 1 min)—are found to be affected by a strong statistical variance; averaged by rain-rate classes, however, the DSDs are well characterized and reproducible (e.g., List 1988; Sauvageot and Lacaux 1995; Nzeukou et al. 2004; Ochou et al. 2007, among others). Most authors agree that because of interactions between drops (coalescence and collisional breakup) falling DSDs evolve toward a kind of ''universal equilibrium'' shape with a constant slope for size larger than the mode and a constant median volume equivalent spherical diameter D_0, as suggested by Srivastava (1978, 1982), List (1988), and Atlas and Ulbrich (2000). This slope is approached only in intense tropical rainfall that enables a large number of drop interactions (e.g., List 1988; Willis and Tattelman 1989; Sauvageot and Lacaux 1995, among others). However, authors also agree that most rainfalls observed at the ground are far from the equilibrium shape and strongly depend on local climatological and dynamic conditions. Notably, for the dynamic conditions, it is acknowledged that, at least for some tropical rain systems, such as squall lines or mesoscale convective systems, where the convective and stratiform components are spatially separated, there are differences between stratiform DSDs—resulting from large snowflakes melting below the 0°C isotherm in the absence of low-level updraft—and convective DSDs—originating from graupel or hail melting in the presence of significant updrafts (e.g., Houze 1993; Sauvageot and Lacaux 1995; Tokay and Short 1996; Yuter and Houze 1997; Atlas et al. 2000; Sauvageot and Koffi 2000; Nzeukou and Sauvageot 2002; Nzeukou et al. 2004). Of course, stratiform rain rates span over a lower range, typically <10 mm h^{-1}, than do convective ones, which can exceed 100 mm h^{-1}. For the same rain rate, stratiform DSDs are made up of larger drops than are convective DSDs. However, as emphasized by several authors (Steiner and Houze 1997; Yuter and Houze 1997; Nzeukou et al. 2004), because convective and stratiform rainfall components are not spatially and statistically distinct, distinguishing between convective and stratiform radar reflectivity factor–rainfall rate (Z–R) relations for rainfall retrieval does not produce results that are significantly better than those from a single Z–R relation. That is why this distinction is not discussed further in this paper. Differences between maritime and continental DSDs have not been discussed.

The goal of this paper is to investigate the way in which the land–ocean storm differences affect the raindrop size distributions and the radar rainfall parameters, from DSD observations gathered in a coastal area, when

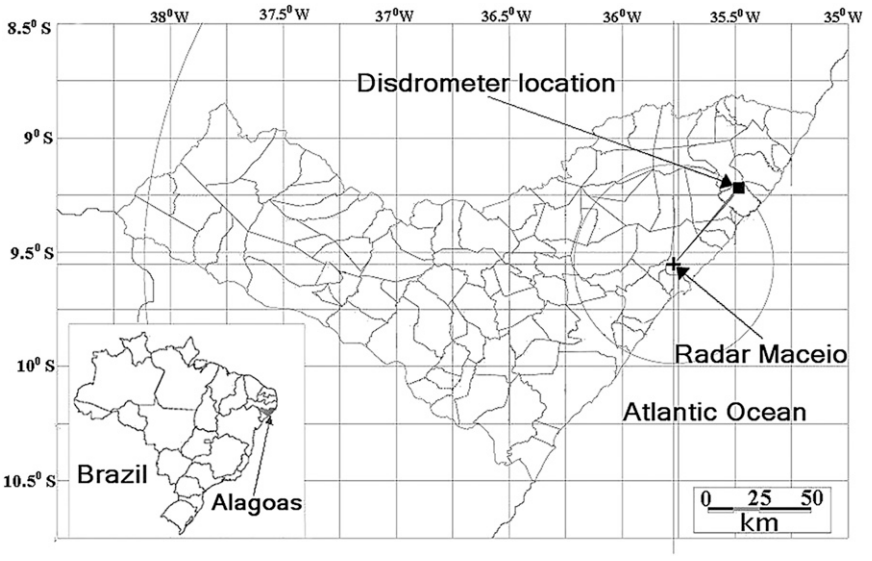

FIG. 1. Location of the disdrometer, 10 km from the shoreline in the northeastern Brazil area.

storms are coming from land (i.e., moving offshore) and from ocean (i.e., moving inshore).

2. Experimental area and dataset

The dataset was collected near Maceió in the state of Alagoas on the northeastern Brazil (NEB) coast (Fig. 1). The experimental area is one of the rainiest in NEB, with an annual rain total of 2000 mm, and its climate is strongly influenced by the warm Atlantic Ocean current (the Brazil Current) (e.g., Martyn 1992; Molion and Bernardo 2002). The wet season is from early March to late September, with rainfall amounting to about 85% of the annual total. There is a ''dry'' season from October to February, with a monthly accumulation of about 70 mm. The general atmospheric circulation is from the southeast (SE) most of the time. The dominance of SE trades over NEB is obvious in the global frequency distribution of lightning and in the percentage of extreme convective events, which are lower east of 40°W longitude and north of 20°S latitude, notably over Alagoas (e.g., Zipser et al. 2006, their Figs. 3, 6, 7, and 8). The large-scale rain-producing mechanisms are frontal systems associated with wavy disturbances carried away within the SE trade wind field (Kousky and Gan 1981; Molion and Bernardo 2002).

During the dry season, when the intertropical convergence zone (ITCZ) is in its southernmost position and when the SE circulation is weak, convective systems can develop over the continent and move eastward, from the continent toward the ocean, over the coastal area. This circulation is marginal for this region but is sufficient, however, to provide the cases of eastward systems used in this study.

DSDs were observed with a Joss and Waldvogel (1967) disdrometer (JWD hereinafter). The JWD enables measurements of the size distribution of raindrops by converting the vertical moment of falling drops into electric pulses. The performances and limitations of these widely used sensors are well known and have been discussed in many papers (e.g., Joss and Waldvogel 1969; Mc Farquhar and List 1993; Sheppard 1990; Sheppard and Joe 1994; Sauvageot and Lacaux 1995; Tokay et al. 2001; Lee and Zawadzki 2005; Cao et al. 2008; see also http://www.distromet.com). Only drops with an equivalent spherical diameter D of larger than 0.3 mm are detected. In the JWD used, the pulses are converted to 8-bit numbers and are sorted according to 20 size classes covering diameters ranging from 0.3 to 5.3 mm. It is acknowledged that, in heavy rainfalls, small drops ($D <$ 1 mm) are not accurately counted with JWD because of instrumental shortcomings. However, Sauvageot and Lacaux (1995) present arguments showing that the relatively low number of small drops usually observed in tropical rain is real when the JWD is carefully used at a site from which the sources of microphonic noise are removed. For tropical rain, low numbers of small drops also are observed by Moumouni et al. (2008) with optical disdrometers. The data were processed for correction of the error due to the dead time of the instrument after the sampling area is hit by a drop by using the method proposed by the manufacturer. Details on the JWD measurement limits are out of the scope of this paper and can be found in the above quoted references. The measurement time span of a DSD is 1 min. Disdrometers are very efficient for the measurement of low rain rates, which is important for an accurate estimation of the mean rain

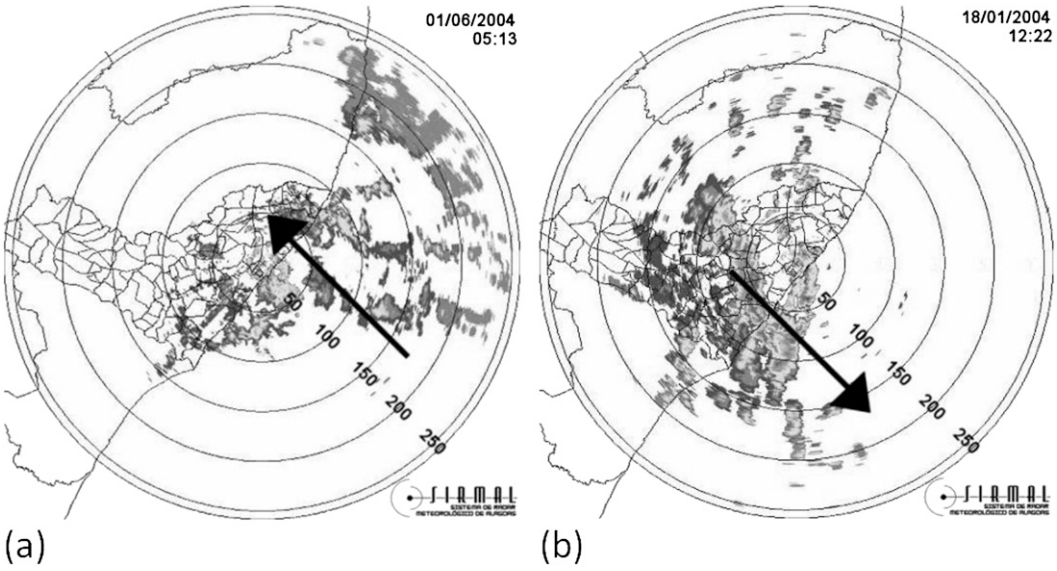

FIG. 2. PPI radar images showing (a) a maritime system, developed over the Atlantic Ocean and moving inshore, and (b) a continental system, developed over the continent and moving offshore. The arrows indicate the direction of motion of the systems.

rate. Knowing DSDs enables the computation of R and the equivalent Z (Joss and Waldvogel 1967; Tenório et al. 2003a,b). Details on the computation of R and Z from DSDs can be found in Doviak and Zrnic (1984, 184–194), Sauvageot (1992, 74–77), and Bringi and Chandrasekar (2001, 406–418), among others. The results on rain accumulation were satisfactorily compared with the measurements of a collocated rain gauge.

Figure 1 shows the location of the JWD, on the Alagoas Atlantic coast, about 40 km north of Maceió. A C-band meteorological radar, located at the Universidade Federal de Alagoas (UFAL), provided a plan position indicator (PPI) of rain systems with a time step of 5 min (Tenório et al. 2003b). This radar is operated by the Sistema de Radar Meteorológico de Alagoas (SIRMAL). The SIRMAL is managed by the Instituto de Ciências Atmosféricas at UFAL. The radar transmits pulses of 2 μs with a peak power of 250 kW and a pulse repetition frequency of 250 Hz. The antenna beamwidth is 2°.

The dataset selected for this study is composed of 25 rainfall events collected in 2004 and 2005. Using PPI radar images as exemplified by Fig. 2, the dataset was divided into two subsets. One is composed of rainfall systems coming from the continent and moving eastward (i.e., offshore), representing the continental subset. The other is composed of rainfall systems developed over the ocean and moving with a westward component, (i.e., inshore), representing the maritime subset. Of course, all of the maritime subset was observed during the wet season whereas the continental one was observed during the ''dry season.''

Table 1 shows the characteristics of the dataset used. For this study, 17 maritime events were selected. They were observed during the rainy season of 2004 (June–September). The entire maritime subset has a total of 4166 min (DSD) representing 69.43 h of rain. For the continental subset, eight events were radar selected; the data were collected during the austral summer of 2004 and 2005. This subset is composed of 1465 min (DSD), which corresponds to 24.41 h of rain. In addition, Table 1 presents the amount of cumulated rain H during the events. Quantitative precipitation estimates by the Maceió radar are not used further because they are out of the scope of this paper.

As pointed out in the introduction, in some studies about rain rate and DSDs a distinction between convective and stratiform precipitation is considered (e.g., Atlas et al. 1990, 1999, 2000; Tokay and Short 1996; Steiner and Houze 1997; Sauvageot and Koffi 2000; Nzeukou et al. 2004; Caracciolo et al. 2008). In the study presented here, a convective–stratiform distinction is not considered because, in frontal systems advected over the Maceió area, convective and stratiform components are

TABLE 1. The dataset; H is the total rain accumulation corresponding to the DSD observations. Each DSD is for a time step of 1 min.

Subset	DSD (No.)	H (mm)
Maritime	4166	323
Continental	1465	66

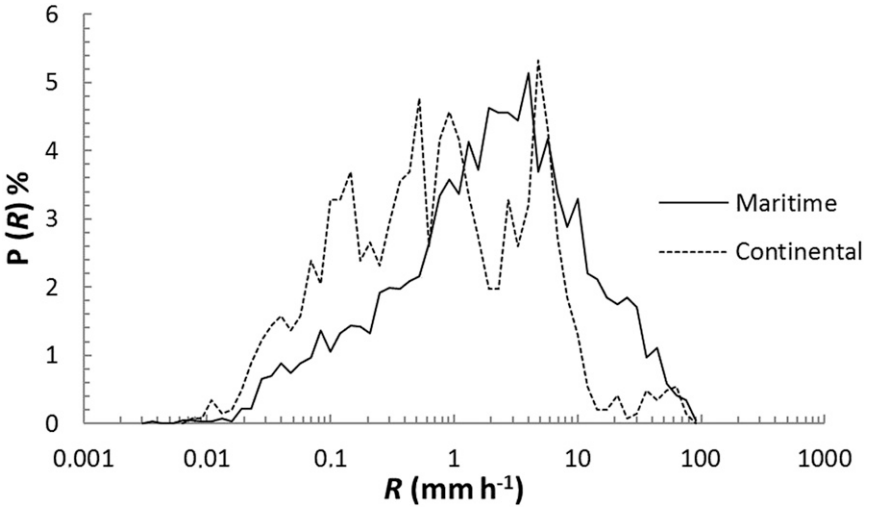

FIG. 3. Probability density of conditional rain rate for the maritime and continental subsets.

not spatially distinct and convection is moderate (see Zipser et al. 2006). In addition, no pertinent data able to justify the discrimination (such as Doppler radar vertical profiler or aircraft in situ measurements) are available and we do not know if the criteria for convective–stratiform distinction are the same for maritime and continental conditions. However, in this paper, most results are given as a function of R, thus enabling us to see the differences between high- and low-rainfall conditions.

3. Results and discussion

Figure 3 shows the probability density function (pdf) of conditional rain rate (i.e., for $R > 0$; e.g., Kedem et al. 1990; Bell and Suhasini 1994) for the two data subsets. The statistical parameters of the curves are given in Table 2. As observed elsewhere for the R distributions (e.g., Atlas et al. 1990; Sauvageot 1994), the pdf shape is close to a lognormal distribution as shown by Fisher's coefficients of skewness (departure from symmetry) and kurtosis (flatness), which are close to zero. The shape of the maritime curve is smoother than the continental one because it is calculated over a larger sample. The two curves are slightly platykurtic and skewed toward the right for maritime and toward the left for continental. However, the important difference is that the conditional mean rain rate of the maritime subset (m_R1 = 4.6 mm h^{-1}) is 44% higher than that of the continental one (m_R2 = 3.2 mm h^{-1}). To verify the statistical significances of the data given in Table 2, a statistical hypothesis test was performed [a Student's t test; see Freund and Perles (2007) for details], using all values of R (maritime and continental), that is, the same data that were used for the pdf calculation. The test results, given in Table 2, disprove the null hypothesis H_0 ($m_R1 = m_R2$) and confirm the alternative hypothesis H_1 ($m_R1 \neq m_R2$). The value found for t is positive and is higher than the critical values (one-tailed and two-tailed), with confidence levels

TABLE 2. Statistical parameters of the probability density function of conditional rain rate for the maritime and continental subsets, and results of Student's t test.

Parameter	Maritime	Continental
Mean m_R (mm h^{-1})	4.6	3.2
Variance σ_R^2 (mm h^{-1})^2	64.8	51.3
Kurtosis	−0.77	−0.98
Skewness	0.61	0.47
Variation coef	1.75	2.24
Student's t test		8.45
Critical value for t (one tailed; confidence level = 0.05)		1.64
(two tailed; confidence level = 0.05)		1.96
(one tailed; confidence level = 0.01)		2.32
(two tailed; confidence level = 0.01)		2.57

of 0.05 and 0.01. Therefore, in rejecting the null hypothesis, the test confirms that the mean rain rate for the maritime subset is significantly greater than the mean rain rate for the continental subset.

Sauvageot (1994) found that, in most continental areas, a correlation is observed between the standard deviation and mean of conditional rain-rate distributions with a variation coefficient CVr ($=\sigma_R/m_R$, where σ_R and m_R are the standard deviation and the mean of R respectively) of close to $5^{1/2}$ ($=2.24$; see also Nzeukou and Sauvageot 2002). In similar work, Short et al. (1993) found, for monsoonal rain observed in coastal areas (Darwin, Australia; Florida) with rain gauges and in the tropical Atlantic with radar, a value of CVr = 5/3 ($=1.67$). The values found for the Maceió area for the continental and the maritime subsets are 2.24 and 1.75, respectively, which are very close to the ones given for continental and maritime/coastal areas in the two quoted references. This result supports the suggestion that the two subsets of Maceió are climatologically different. In addition, if the pdf is lognormal and CVr is constant, the knowledge of only one parameter (mean or variance) of the distribution is enough to determine the pdf (Sauvageot 1994).

To understand the cause of these differences, the DSDs have been considered. Figure 4 presents averaged DSDs for the continental and maritime subsets, using several rain-rate classes for DSD averaging [such as done by Sauvageot and Lacaux (1995)]. The curves of Fig. 4 exhibit some irregularities in the form of peaks located around equivalent spherical diameters of 0.6–0.7, 1.0–1.2, and 1.8–2.1 mm. It is well known and demonstrated (McFarquhar and List 1993) that these peaks are entirely instrument related. They are due to small irregularities of the transfer function of the electronic circuits. These irregularities are permanent and only modify the distribution of the drops between some classes of fixed sizes.

If one ignores these irregularities, Fig. 4 shows that maritime DSDs are composed of a larger number of drops than are continental ones. The difference is a maximum around the mode of the DSDs and decreases on the right, the side of the large drops. For $R <$ 10 mm h^{-1} the difference is for the small drops. As R increases, the difference moves toward the large drops. For D larger than about 2 mm, the drop number is higher for continental rain.

To quantify these differences in drop number and DSD shape between maritime and continental, individual DSDs (i.e., at the time step of 1 min) have been fitted to an analytic form. Tropical DSDs are usually fitted using gamma-modified (e.g., Ulbrich 1983) or lognormal (e.g., Sauvageot and Lacaux 1995) forms. The two forms give a very good fitting. We have used the lognormal form because the parameters of the fitting are independent from each other, which is not the case with the gamma-modified form. The lognormal distribution has the following expression (e.g., Crow and Shimizu 1988):

$$N(D) = \frac{N_T}{(2\pi)^{0.5}(\ln\sigma)D} \times \exp[-\ln^2(D/D_g)/(2\ln^2\sigma)], \tag{1}$$

where N_T is the total number of drops, D_g is the mean geometrical spherical diameter, and σ is the standard geometrical deviation of D as respectively expressed by

$$N_T = \int_0^\infty N(D)\, dD, \tag{2}$$

$$\ln D_g = \overline{\ln D}, \quad \text{and}, \tag{3}$$

$$\ln^2\sigma = \overline{(\ln D - \ln D_g)^2}. \tag{4}$$

The results of the fitting are given in Table 3. They confirm and enlarge what appears in Fig. 4. For rain rates lower than 10 mm h^{-1}, which includes most of the rain rates observed over the studied area, the drop number in maritime rain is about 2 times that in continental rain. The mean drop size D_g and the standard deviation σ of DSDs are smaller for maritime than for continental subsets (by 11% for D_g and 8% for σ). However, one observes that the differences between rainfall DSD parameters decrease as the rainfall rate increases above about 10 mm h^{-1} (Fig. 4; Table 3). With the purpose of verifying the statistical significances of the parameters given in Table 3, a statistical test (Student's t test) was applied to the same maritime and continental dataset used to plot Fig. 4. The results of the test are given in Table 4. Since the value of t, for the first four intervals and for all intervals, is positive and is higher than the critical values, the null hypothesis H_0 (maritime = continental) should be rejected. The alternative hypothesis H_1 (maritime $\neq$ continental) is confirmed. For the interval $R > 40$ mm h^{-1}, the value of t is also positive but is smaller than the critical value and therefore in this case the alternative hypothesis H_1 should be rejected, generating a possibility of equal means. Thus, except for $R > 40$ mm h^{-1}, the parameters given in Table 3 for maritime and continental can be considered to be statistically different.

To emphasize the difference for the drop number, Fig. 5 displays N_t as a function of R. Figures 5a and 5b show the data points for the individual DSDs and the fitted curves separately for the two subsets for clarity. The two fitted curves are shown together in Fig. 5c for comparison.

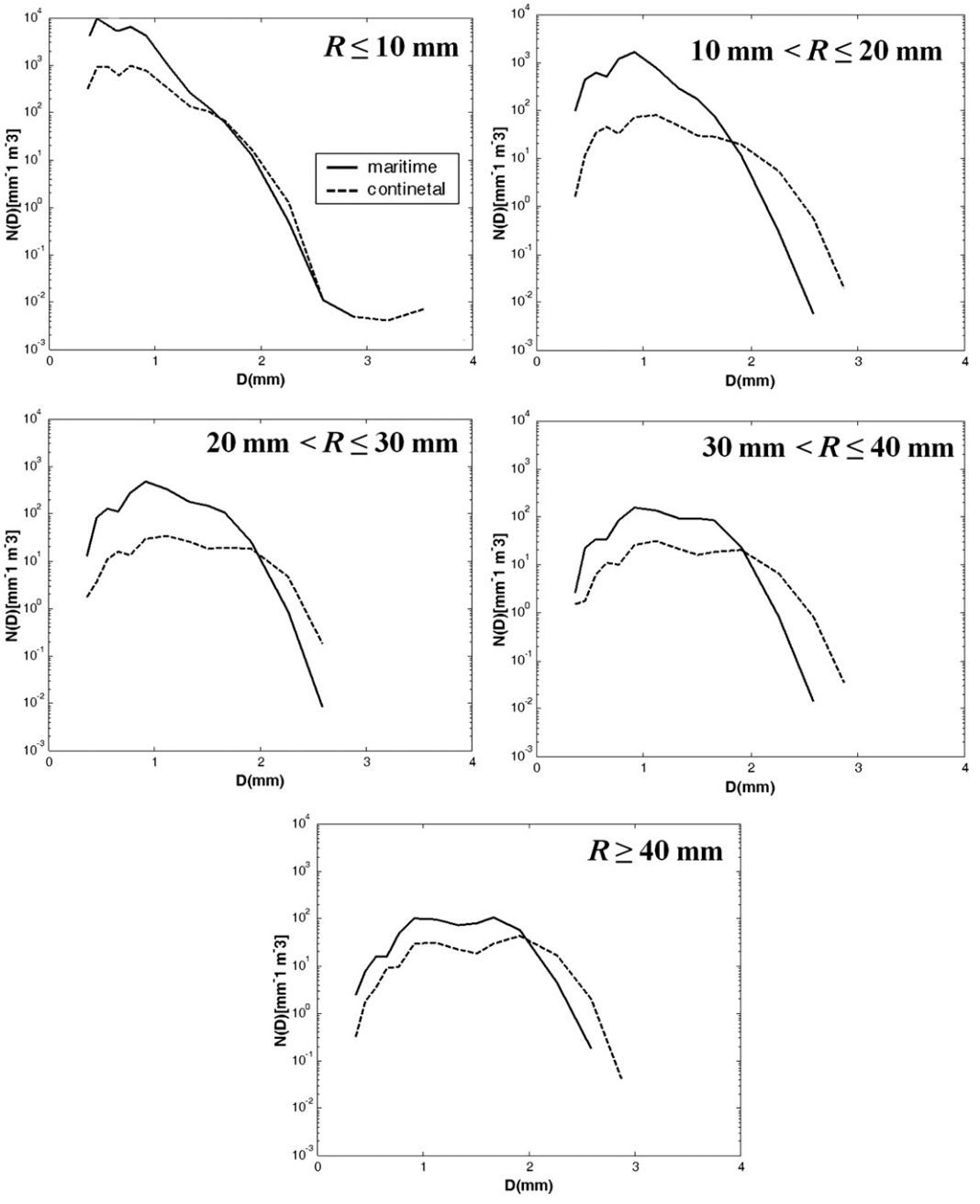

FIG. 4. Raindrop size distributions averaged over five rain-rate classes.

For the continental subset, the curve fits the data points for all of the observed values of R and notably between 10 and 100 mm h^{-1}. For the maritime subset, the cloud of data points bends below the fitted curve for $R >$ 10 mm h^{-1}.

The decrease of the difference between the maritime and continental DSDs parameters for $R > 10$ mm h^{-1} suggests that, as convection intensifies, convective clouds over land and over sea become more and more similar. In the microphysical processes leading to the DSDs observed at the ground, the dynamical constraints of convection become more important in comparison with the conditions at ground and at low atmospheric levels.

The equations of the curves fitted to the data points in Fig. 5 are

$$N_t(R) = 221R^{0.61}, \tag{5}$$

TABLE 3. Parameters of the lognormal curves fitted to the averaged DSDs of Fig. 4. Here N_t, D_g, and σ are the total drop number, the mean geometrical spherical diameter, and the standard geometrical deviation of D, respectively.

Class of rain rate (mm h^{-1})	Maritime			Continental		
	N_t (m^{-3})	D_g (mm)	σ	N_t (m^{-3})	D_g (mm)	σ
$R \leq 10$	578	1.02	1.27	358	1.13	1.37
$10 < R \leq 20$	892	1.39	1.48	783	1.26	1.46
$20 < R \leq 30$	951	1.40	1.60	896	1.41	1.56
$30 < R \leq 40$	1008	1.57	1.69	1018	1.45	1.60
$R > 40$	889	1.92	1.33	1156	1.68	1.45
All	460	1.09	0.85	203	1.17	1.01

with $r = 0.90$, for maritime and

$$N_t(R) = 105R^{0.66}, \tag{6}$$

with $r = 0.93$, for continental. Here, r is the correlation coefficient, N_t is in inverse meters cubed, and R is in millimeters per hour.

Differences in drop size distribution have an influence on the radar parameters and notably on the Z–R relation used to convert radar reflectivity factor to rain rate. This relation is written $Z = aR^b$, where a and b are coefficients (e.g., Atlas et al. 1999, among others). Figure 6 shows the plots of Z–R data points for the individual DSDs and the curves $Z = aR^b$ fitted by linear regression to the data points. For clarity, the maritime and continental data points are plotted separately. Using the numerical values obtained from the fitting, the Z–R relations are

$$Z = 146R^{1.28}, \tag{7}$$

with $r = 0.98$, for maritime rain and

$$Z = 256R^{1.27}, \tag{8}$$

with $r = 0.98$, for continental rain, where r is the correlation coefficient; Z is in millimeters to the sixth power per meter cubed, and R is in millimeters per hour.

For northeastern coastal Brazil, the power coefficient b is found to be almost constant, at approximately 1.27, which is a value that is observed in many places in the tropical area [e.g., Hudlow (1979): $Z = 227R^{1.25}$ for the Global Atlantic Tropical Experiment (GATE); Rosenfeld et al. (1993): $Z = 230R^{1.25}$ for the Darwin area; and Atlas et al. (2000): $Z = 216R^{1.25}$ for Kapingamarangi Atoll]. The Z–R curves for maritime and continental subsets are almost parallel. The only difference is found in coefficient a, which is about 2 times as high for the continental as for the maritime subset. Inside each type, a distinction between rain rate higher and lower than 10 mm h^{-1} (tentatively representing convective and stratiform rain) shows that the linear coefficient a is higher for $R > 10$ mm h^{-1} than for $R < 10$ mm h^{-1} as usually observed at tropical latitudes (e.g., Yuter and Houze 1997; Tokay et al. 2001).

TABLE 4. Results of Student's t test. Here 0.05 and 0.01 indicate the confidence levels.

Class of rain rate (mm h^{-1})	t	Critical value for t			
		One tailed		Two tailed	
		0.05	0.01	0.05	0.01
$R \leq 10$	43.14	1.64	2.32	1.96	2.57
$10 < R \leq 20$	17.29	1.66	2.37	1.99	2.64
$20 < R \leq 30$	6.42	1.69	2.44	2.03	2.73
$30 < R \leq 40$	5.19	1.70	2.47	2.05	2.77
$R > 40$	0.32	1.66	2.37	1.99	2.64
All	47.57	1.64	2.32	1.96	2.57

4. Conclusions

Continental and maritime convective storm systems display some significant differences. Are these

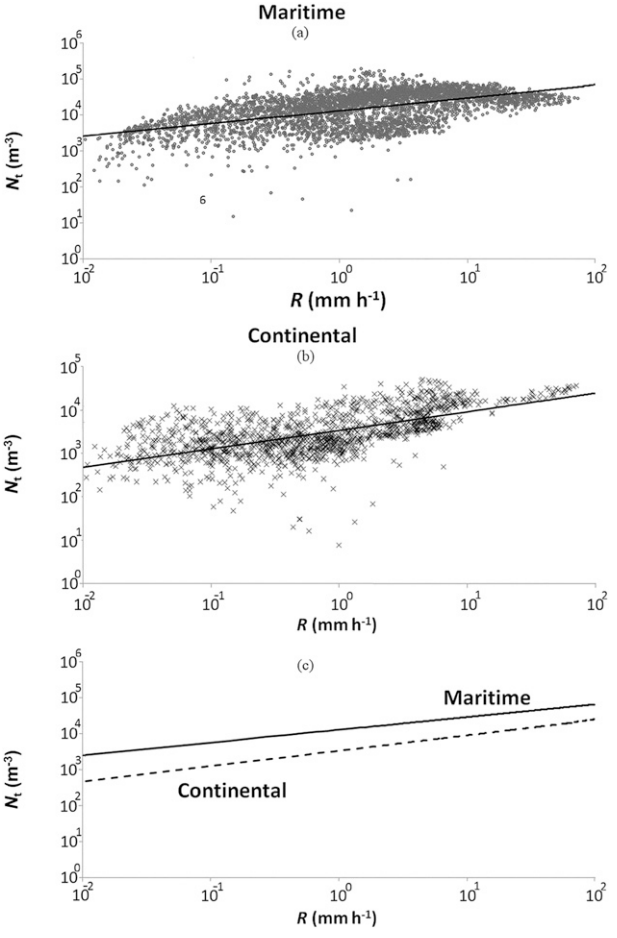

FIG. 5. Data points and fitted curves for the total drop number by drop size distribution N_t vs rain rate for (a) maritime and (b) continental data subsets. (c) The two curves shown together.

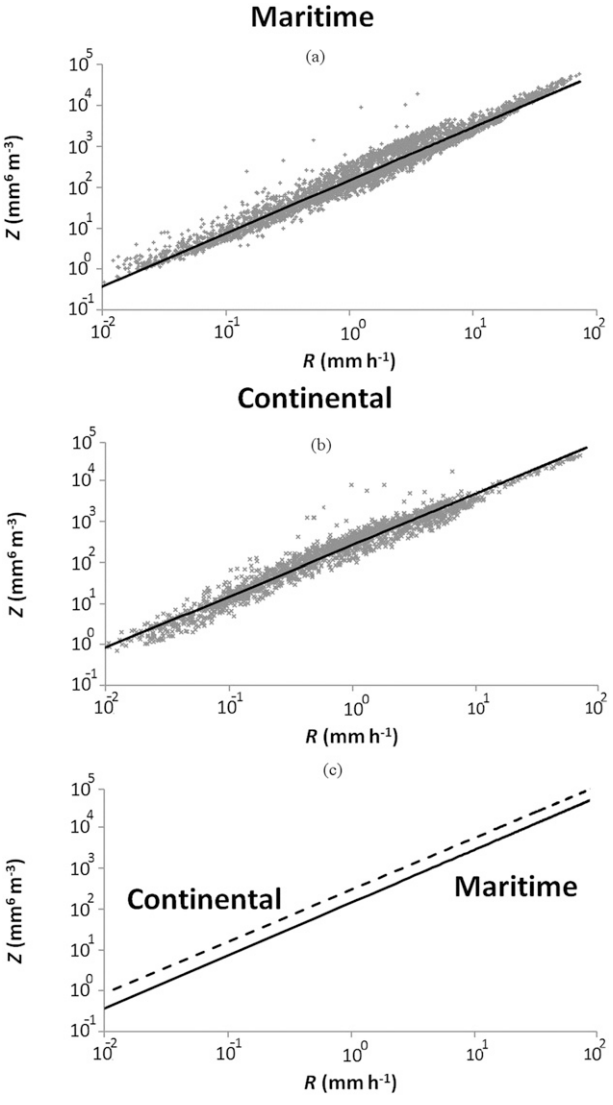

FIG. 6. Data points and fitted curves for Z–R relation for (a) maritime and (b) continental data subsets. (c) For clarity, the two curves are shown together.

differences perceptible on the characteristics and radar parameters of rainfall observed over a coastal area where the atmospheric circulation can be inshore or offshore? To answer this question, a dataset of DSDs has been gathered from a coastal site of northeastern Brazil. This dataset has been segmented into two subsets: systems moving inshore and offshore, representing the maritime and continental subsets, respectively. DSDs were used to calculate rain rate and radar reflectivity factor. The parameters of the lognormal fitting of individual DSDs were also calculated—notably N_t, the DSD drop number.

The probability density function of conditional rain rate is approximately lognormal for the two subsets, but the mean conditional rain rate is found to be larger for maritime cases (4.6 mm h^{-1}) than for continental ones (3.2 mm h^{-1}). The variation coefficient of rain rate is found to be approximately 2.24 for the continental subset and 1.75 for the maritime one. For a same rain rate, the total number of drops of individual DSDs is higher by about a factor of 2 for maritime than for continental DSDs. However, this difference reduces for $R >$ 10 mm h^{-1}, suggesting that the microphysics of convective clouds over sea and over land become more similar when convection intensifies. Drop sizes are thus smaller in maritime rain than in continental rain for rain rates lower than 10 mm h^{-1}. As a result, the radar reflectivity of maritime rain is lower than that of continental rain. The reflectivity–rain-rate relation is $Z = 146R^{1.27}$ for maritime rain and $Z = 256R^{1.27}$ for continental rain. For northeastern coastal Brazil, the power coefficient b is found to be practically constant, around 1.27—a value observed in many places in the tropical area. In fact, the two coefficients of Eq. (8) are remarkably similar to those observed for all R by Hudlow (1979) at $Z = 227R^{1.25}$ for GATE, Rosenfeld et al. (1993) at $Z = 230R^{1.25}$ for the Darwin area, and Atlas et al. (2000) at $Z = 216R^{1.25}$ for Kapingamarangi Atoll.

In conclusion, this work illustrates that the parameters of rainfall observed on the coast of Alagoas state in northeastern Brazil are different for rainfall generated by cloud systems moving inshore and for those moving offshore. Consequently, for rainfall retrieval from radar data gathered from the coast of northeastern Brazil around Alagoas, better estimates will be obtained if separate Z–R relations are used for rain-bearing systems that are moving inshore and offshore. It is suggested that this result deserves to be investigated for other coastal sites where the atmospheric circulation changes with respect to the direction of the coast.

Acknowledgments. We acknowledge the Conselho Nacional de Desenvolvimento Científico e Tecnológico (CNPq) and Coordenação de Aperfeiçoamento de Pessoal de Nível Superior (CAPES) for partial financial support.

REFERENCES

Atlas, D., and C. W. Ulbrich, 2000: An observationally based conceptual model of warm oceanic convective rain in the tropics. *J. Appl. Meteor.,* **39,** 2165–2181.

——, D. Rosenfeld, and D. A. Short, 1990: The estimation of convective rainfall by area integrals. 1. The theoretical and empirical basis. *J. Geophys. Res.,* **95,** 2153–2160.

——, C. W. Ulbrich, F. D. Marks Jr., E. Amitai, and C. R. Williams, 1999: Systematic variation of drop size and radar–rainfall relations. *J. Geophys. Res.,* **104,** 6155–6169.

——, ——, ——, R. A. Black, E. Amitai, P. T. Willis, and C. E. Samsury, 2000: Partitioning tropical oceanic convective and stratiform rains by draft strength. *J. Geophys. Res.,* **105,** 2259–2267.

Bell, T. L., and R. Suhasini, 1994: Principal modes of variation of rain-rate probability distributions. *J. Appl. Meteor.,* **33,** 1067–1078.

Black, R. A., and J. Halett, 1986: Observations of the distribution of ice in hurricanes. *J. Atmos. Sci.,* **43,** 802–822.

Bringi, K. N., and V. Chandrasekar, 2001: *Polarimetric Doppler Weather Radar*. Cambridge University Press, 636 pp.

Cao, Q., G. Zhang, E. Brandes, T. Schuur, A. Ryzhkov, and K. Ikeda, 2008: Analysis of video disdrometer and polarimetric radar to characterize rain microphysics in Oklahoma. *J. Appl. Meteor. Climatol.,* **47,** 2238–2255.

Caracciolo, C., F. Porcu, and F. Prodi, 2008: Precipitation classification at mid-latitudes in terms of drop size distribution parameters. *Adv. Geosci.,* **16,** 11–17.

Christian, H. J., and Coauthors, 2003: Global frequency and distribution of lightning as observed from space by the Optical Transient Detector. *J. Geophys. Res.,* **108,** 4005, doi:10.1029/2002JD002347.

Crow, E. L., and K. Shimizu, 1988: *Lognormal Distributions*. Dekker, 387 pp.

Doviak, R. J., and D. Zrnic, 1984: *Doppler Radar and Weather Observations*. Academic Press, 458 pp.

Freund, J. E., and B. M. Perles, 2007: *Modern Elementary Statistics*. 12th ed. Prentice Hall, 561 pp.

Gebremichael, M., W. F. Krajewski, T. M. Over, Y. N. Takayabu, P. Arkin, and M. Katayama, 2008: Scaling of tropical rainfall as observed by TRMM precipitation radar. *Atmos. Res.,* **88,** 337–354.

Houze, R. A., 1993: *Cloud Dynamics*. Academic Press, 570 pp.

Hudlow, M. D., 1979: Mean rainfall patterns for the three phases of GATE. *J. Appl. Meteor.,* **18,** 1656–1669.

Joss, J., and A. Waldvogel, 1967: Ein Spectrograph für Niederschlagstropfen mit automatisher Auswertung (A spectrograph for the automatic analysis of raindrops). *Pure Appl. Geophys.,* **68,** 240–246.

——, and ——, 1969: Raindrop size distribution and sampling size errors. *J. Atmos. Sci.,* **26,** 566–569.

Kedem, B., L. S. Chiu, and G. R. North, 1990: Estimation of mean rain rate: Application to satellite observations. *J. Geophys. Res.,* **95,** 1965–1972.

Kousky, V. E., and M. A. Gan, 1981: Upper tropospheric cyclonic vortices in the tropical South Atlantic. *Tellus,* **33,** 538–551.

Kummerow, C., W. Barnes, T. Kozu, J. Shine, and J. Simpson, 1998: The Tropical Rainfall Measuring Mission (TRMM) sensor package. *J. Atmos. Oceanic Technol.,* **15,** 809–817.

Lee, G., and I. Zawadzki, 2005: Variability of drop size distributions: Noise and noise filtering in disdrometric data. *J. Appl. Meteor.,* **44,** 634–652.

List, R., 1988: A linear radar reflectivity–rainrate relationship for steady tropical rain. *J. Atmos. Sci.,* **45,** 3564–3572.

Liu, C., and E. J. Zipser, 2005: Global distribution of convection penetrating the tropical tropopause. *J. Geophys. Res.,* **110,** D23104, doi:10.1029/2005JD006063.

——, ——, D. J. Cecil, S. W. Nesbitt, and S. Sherwood, 2008: A cloud and precipitation feature database from nine years of TRMM observations. *J. Appl. Meteor. Climatol.,* **47,** 2712–2728.

Martyn, D., 1992: *Climates of the World*. Elsevier, 435 pp.

McFarquhar, G. M., and R. List, 1993: The effect of curve fits for the disdrometer calibration on raindrop spectra, rainfall rate and radar reflectivity. *J. Appl. Meteor.,* **32,** 774–782.

Molion, L. C. B., and S. O. Bernardo, 2002: Uma revisão da dinâmica das chuvas no Nordeste do Brasil (A review of the dynamics of rainfall over northeastern Brazil). *Braz. J. Meteor.,* **17,** 1–10.

Moumouni, S., M. Gosset, and E. Hougninou, 2008: Main features of rain drop size distributions observed in Benin, West Africa, with optical disdrometers. *Geophys. Res. Lett.,* **35,** L23807, doi:10.1029/2008GL035755.

Munchak, S. J., and A. Tokay, 2008: Retrieval of raindrop size distribution from simulated dual-frequency radar measurements. *J. Appl. Meteor. Climatol.,* **47,** 223–239.

Nesbitt, S. W., and E. J. Zipser, 2003: The diurnal cycle of rainfall and convective intensity according to three years of TRMM measurements. *J. Climate,* **16,** 1456–1475.

Nzeukou, A., and H. Sauvageot, 2002: Distribution of rainfall parameters near the coast of France and Senegal. *J. Appl. Meteor.,* **41,** 69–82.

——, ——, A. D. Ochou, and C. M. F. Kebe, 2004: Raindrop size distribution and radar parameters at Cape Verde. *J. Appl. Meteor.,* **43,** 90–105.

——, ——, and L. Féral, 2006: Rain rate and attenuation statistics along paths in a tropical coastal area from radar data. *Radio Sci.,* **41,** RS2005, doi:10.1029/2004RS003227.

Ochou, A. D., A. Nzeukou, and H. Sauvageot, 2007: Parametrization of drop size distribution with rain rate. *Atmos. Res.,* **84,** 58–66.

Orville, R. E., and R. W. Henderson, 1986: Global distribution of midnight lightning: September 1977 to August 1978. *Mon. Wea. Rev.,* **114,** 2640–2653.

Rosenfeld, D., D. Wolf, and D. Atlas, 1993: General probability-matched relations between radar reflectivity and rain rate. *J. Appl. Meteor.,* **32,** 50–72.

Sall, S. M., and H. Sauvageot, 2005: Cyclogenesis off the African coast: The case of Cindy in August 1999. *Mon. Wea. Rev.,* **133,** 2803–2813.

——, ——, A. T. Gaye, A. Viltard, and P. de Felice, 2006: A cyclogenesis index for tropical Atlantic off the African coasts. *Atmos. Res.,* **79,** 123–147.

Sauvageot, H., 1992: *Radar Meteorology*. Artech House, 366 pp.

——, 1994: The probability density function of rain rate and the estimation of rainfall by area integrals. *J. Appl. Meteor.,* **33,** 1255–1262.

——, and J. P. Lacaux, 1995: The shape of averaged drop size distributions. *J. Atmos. Sci.,* **52,** 1070–1083.

——, and M. Koffi, 2000: Multimodal raindrop size distributions. *J. Atmos. Sci.,* **57,** 2480–2492.

Seity, Y., S. Soula, and H. Sauvageot, 2000: Radar observation and lightning detection in coastal thunderstorms. *Phys. Chem. Earth,* **25,** 1107–1110.

——, ——, and ——, 2001: Lightning and precipitation relationship in coastal thunderstorms. *J. Geophys. Res.,* **106,** 22 801–22 816.

Sheppard, B. E., 1990: Effect of irregularities in the diameter classification of raindrops by the Joss–Waldvogel disdrometer. *J. Atmos. Oceanic Technol.,* **7,** 180–183.

——, and P. I. Joe, 1994: Comparison of raindrop size distribution measurements by a Joss–Waldvogel disdrometer, a PMS 2DG spectrometer, and a POSS Doppler radar. *J. Atmos. Oceanic Technol.,* **11,** 874–887.

Short, D. A., D. B. Wolf, D. Rosenfeld, and D. Atlas, 1993: A study of the threshold method utilizing raingage data. *J. Appl. Meteor.,* **32,** 1379–1387.

Srivastava, R. C., 1978: Parameterization of raindrop size distributions. *J. Atmos. Sci.,* **35,** 108–117.

——, 1982: A simple model of particle coalescence and breakup. *J. Atmos. Sci.,* **39,** 1317–1322.

Steiner, M., and R. A. Houze, 1997: Sensitivity of the estimated monthly convective rain fraction to the choice of *Z–R* relation. *J. Appl. Meteor.,* **36,** 452–462.

Tenório, R. S., L. C. B. Molion, H. Sauvageot, D. A. Quintão, and M. A. Antonio, 2003a: Radar rainfall studies over the eastern coast of Northeast Brazil. *Extended Abstracts, 31st Int. Conf. on Radar Meteorology,* Seattle, WA, Amer. Meteor. Soc., P3B.1. [Available online at https://ams.confex.com/ams/pdfpapers/64394.pdf.]

——, M. C. S. Moraes, D. A. Quintão, and B. H. Kwon, 2003b: Estimation of the *Z–R* relation through the disdrometer for the coastal region in the northeast of Brazil. *J. Kor. Earth Sci. Soc.,* **24,** 30–35.

Tokay, A., and D. A. Short, 1996: Evidence from tropical raindrop spectra of the origin of rain from stratiform versus convective clouds. *J. Appl. Meteor.,* **35,** 355–371.

——, ——, C. R. Williams, W. L. Eckland, and K. S. Gage, 1999: Tropical rainfall associated with convective and stratiform clouds: Intercomparison of disdrometer and profiler measurements. *J. Appl. Meteor.,* **38,** 302–320.

——, A. Kruger, and W. E. Krajewski, 2001: Comparison of drop size distribution measurements by impact and optical disdrometers. *J. Appl. Meteor.,* **40,** 2083–2097.

Ulbrich, C. W., 1983: Natural variations in the analytical form of the raindrop size distribution. *J. Climate Appl. Meteor.,* **22,** 1764–1775.

Willis, P. T., and P. Tattelman, 1989: Drop-size distribution associated with intense rainfall. *J. Appl. Meteor.,* **28,** 3–15.

Yuter, S. E., and R. A. Houze, 1997: Measurements of raindrop size distributions over the Pacific warm pool and implications for *Z–R* relations. *J. Appl. Meteor.,* **36,** 847–867.

Zipser, E. J., and K. R. Lutz, 1994: The vertical profile of radar reflectivity of convective cells: A strong indicator of storm intensity and lightning probability? *Mon. Wea. Rev.,* **122,** 1751–1759.

——, D. J. Cecil, C. Liu, S. W. Nesbitt, and D. P. Yorty, 2006: Where are the most intense thunderstorms on Earth? *Bull. Amer. Meteor. Soc.,* **87,** 1057–1071.